

Nonequilibrium dynamics of condensates in a lattice with the two-particle-irreducible effective action in the $1/\mathcal{N}$ expansion

Kristan Temme* and Thomas Gasenzer†

Institut für Theoretische Physik, Universität Heidelberg, Philosophenweg 16, 69120 Heidelberg, Germany

(Received 21 June 2006; published 2 November 2006)

The dynamical evolution of a Bose-Einstein condensate trapped in a one-dimensional lattice potential is investigated theoretically in the framework of the Bose-Hubbard model. The emphasis is set on the far-from-equilibrium evolution in a case where the gas is strongly interacting. This is realized by an appropriate choice of the parameters in the Hamiltonian, and by starting with an initial state, where one lattice well contains a Bose-Einstein condensate while all other wells are empty. Oscillations of the condensate as well as noncondensate fractions of the gas between the different sites of the lattice are found to be damped as a consequence of the collisional interactions between the atoms. Functional integral techniques involving self-consistently determined mean fields as well as two-point correlation functions are used to derive the two-particle-irreducible (2PI) effective action. The action is expanded in inverse powers of the number of field components \mathcal{N} , and the dynamic equations are derived from it to next-to-leading order in this expansion. This approach reaches considerably beyond the Hartree-Fock-Bogoliubov mean-field theory, and its results are compared to the exact quantum dynamics obtained by Rey *et al.* [Phys. Rev. A **69**, 033610 (2004)] for small atom numbers.

DOI: [10.1103/PhysRevA.74.053603](https://doi.org/10.1103/PhysRevA.74.053603)

PACS number(s): 03.75.Kk, 03.75.Lm, 03.70.+k, 05.70.Ln

I. INTRODUCTION

The dynamical evolution of ultracold atomic quantum gases driven far out of equilibrium are a subject of intensely growing interest. Precision measurement techniques for many-body observables have been and are being developed with vigorous effort. This technology has triggered a strong demand for progress in theoretically describing nonequilibrium quantum many-body dynamics of strongly interacting systems beyond mean-field approximations. Recent highlights of this development include, e.g., the variation and enhancement of the atomic interactions on the basis of Feshbach scattering resonances [1–5] as well as the achievement of strongly correlated regimes within optical lattices [6,7]. With these techniques, e.g., a Bose-Einstein condensate can suddenly be brought out of equilibrium, so that mean-field approximations such as chosen in Gross-Pitaevskii and Hartree-Fock-Bogoliubov theory no longer suffice to describe its time-evolution.

Mean-field approximations are valid as long as both classical statistical and quantum fluctuations are small. This is, in general, only the case in situations close to equilibrium. But even close to equilibrium, fluctuations can play an important role on long time scales. For example, the long-time evolution towards the Bose-Einstein equilibrium state relies on the fluctuations appearing beyond mean-field order in a quantum many-body description.

Moreover, kinetic descriptions beyond mean-field order which have been studied intensely in the past (in the context of cold atomic gases, cf., e.g., Refs. [8–17] and references therein), usually neglect the initial dynamics directly after the change in the boundary conditions which drive the system out of equilibrium. This shortcoming is cured in dynamical

approaches in which coupled equations of motion for the correlation functions are derived to describe the time evolution starting from a specific initial state. The buildup of correlations beyond mean-field order, in these equations, is usually taken into account by means of non-Markovian integrations over the evolution history of the correlation functions, see, e.g., [18–23].

In this paper we consider the time evolution of a Bose-Einstein condensate trapped in a one-dimensional lattice potential in the framework of the Bose-Hubbard model. The emphasis is set on the far-from-equilibrium evolution in a case where the gas is strongly interacting. This is realized by an appropriate choice of the parameters in the Hamiltonian. In the nonequilibrium initial state one lattice well contains a Bose-Einstein condensate while all other wells are empty. At NIST, such a system has recently been realized in experiment [24]. Theoretically, it has been considered, e.g., in Refs. [22,25,26], using approximations beyond mean-field order.

We find oscillations of the condensed as well as the noncondensed fractions of the gas between the different sites of the lattice. These oscillations are damped as a consequence of the collisional interactions between the atoms. Our theoretical approach is based on functional integral techniques involving self-consistently determined mean fields as well as two-point correlation functions. Specifically, the dynamic equations are derived from the two-particle-irreducible (2PI) effective action [27–29]. Any approximations necessary in practice are made at the level of this action before the dynamic equations are derived by functional differentiation. This ensures crucial symmetries like total particle number and energy to be automatically conserved. The 2PI effective action has been used to compare various perturbative approximations with the exact result for the dynamics of a strongly correlated one-dimensional lattice Bose gas [22]. The approach yields dynamic equations which constitute a proper initial-value problem and therefore are in principle valid over all times, including initial and long-term evolu-

*Email address: k.temme@thphys.uni-heidelberg.de

†Email address: t.gasenzer@thphys.uni-heidelberg.de

tion. In the Markovian limit, in which their validity is restricted to certain intermediate times, the well-known kinetic theory descriptions including the Gross-Pitaevskii and Bogoliubov–de Gennes equations as well as Landau and Beliaev quasiparticle damping can be rederived from these dynamic equations [16,17].

In this paper we consider a nonperturbative approximation which reaches substantially beyond the Hartree-Fock-Bogoliubov mean-field theory. This nonperturbative approach is based on a systematic expansion of the 2PI effective action in powers of the inverse number of field components \mathcal{N} [19,30]. We point out that this $1/\mathcal{N}$ expansion of the 2PI effective action goes substantially beyond and is not to be confused with the standard $1/\mathcal{N}$ expansion of the 1PI effective action. For example, it can be used to calculate critical exponents characterizing correlation functions in the vicinity of a phase transition, even in the limit of vanishing \mathcal{N} [31]. The 2PI $1/\mathcal{N}$ expansion has recently been used to describe the dynamics of an ultracold atomic Bose gas far from equilibrium [23]. We compare our results to the exact quantum dynamics also obtained in Ref. [22] for small atom numbers.

The 2PI $1/\mathcal{N}$ expansion to next-to-leading order yields dynamic equations which contain direct scattering, memory, and “off-shell” effects. It allows one to describe far-from-equilibrium dynamics as well as the late-time approach to quantum thermal equilibrium. Recently, these methods have allowed important progress in describing the dynamics of strongly interacting relativistic systems far from thermal equilibrium for bosonic [19,32–37] as well as fermionic degrees of freedom [38,39]. In Ref. [40], the predictions from the 2PI approach for a classical gas were compared with simulations of classical equations of motion, which showed that the NLO $1/\mathcal{N}$ approximation for this case gives very good results already for $\mathcal{N}=2$.

Our paper is organized as follows: In Sec. II we recall the functional description of the quantum many-body dynamics and present the set of coupled dynamic equations for the mean field and the two-point correlation functions. We discuss consequences of this distinction for the self-energies which quantify the beyond-HFB contributions in the dynamic equations for the correlation functions. In Sec. III we present numerical results for the nonequilibrium dynamics in a one-dimensional lattice potential and compare these to the results from corresponding exact calculations. Our conclusions are drawn in Sec. IV.

II. THE 2PI EFFECTIVE ACTION APPROACH TO THE DYNAMICS OF A LATTICE BOSE GAS

We study a nonrelativistic system characterized by the Bose-Hubbard Lagrangian

$$\begin{aligned} \mathcal{L}(n,t) = & \frac{i}{2} [\Psi_n^*(t) \partial_t \Psi_n(t) - \Psi_n(t) \partial_t \Psi_n^*(t)] \\ & + J [\Psi_n^*(t) \Psi_{n+1}(t) + \Psi_{n+1}^*(t) \Psi_n(t)] \\ & - \epsilon_n \Psi_n^*(t) \Psi_n(t) - \frac{U}{2} [\Psi_n^*(t) \Psi_n(t)]^2. \end{aligned} \quad (1)$$

Here, Ψ is a complex-valued, i.e., two-component, field defined in time t and at site n of the one-dimensional lattice. We use units where $\hbar=1$. J is the coupling which depends on the hopping probability and therefore on the lattice depth, ϵ_i denotes an external potential, and U a real-valued coupling constant. Only local interactions, between atoms at one lattice site, are taken into account.

A. Generating functional for correlation functions

The functional integral formulation of the quantum dynamics of a Bose-Einstein gas has been discussed extensively in the literature. For details we refer to our recent discussion [23] of the nonperturbative effective-action approach to far-from-equilibrium dynamics of an ultracold Bose gas. To simplify our notation we will, in the following, change to a representation of the field Ψ in terms of its real and imaginary parts, i.e.,

$$\Phi_1 = \sqrt{2} \operatorname{Re} \Psi, \quad \Phi_2 = \sqrt{2} \operatorname{Im} \Psi, \quad (2)$$

such that $\Psi = (\Phi_1 + i\Phi_2) / \sqrt{2}$. Furthermore, we include the lattice index n into the argument of the field $\Phi_i(x)$, i.e., $x = (t, n) \equiv (x_0, n)$.

The time evolution of quantum correlation functions can be derived from a generating functional. This involves fields $\hat{\Phi}_i$ obeying Bose commutation relations $[\hat{\Phi}_i(t, \vec{x}), \hat{\Phi}_j(t, \vec{y})] = -\sigma_{2,ij} \delta(\vec{x} - \vec{y})$, where σ_2 denotes the Pauli 2-matrix, as well as the nonequilibrium normalized initial-state density matrix $\hat{\rho}_D(t_0)$:

$$\begin{aligned} Z[J, K; \hat{\rho}_D] = & \operatorname{Tr} \left[\hat{\rho}_D(t_0) \mathcal{T}_C \exp \left\{ i \int_{x,C} \hat{\Phi}_i(x) J_i(x) \right. \right. \\ & \left. \left. + \frac{i}{2} \int_{xy,C} \hat{\Phi}_i(x) K_{ij}(x, y) \hat{\Phi}_j(y) \right\} \right], \end{aligned} \quad (3)$$

where $\int_x \equiv \int_0^\infty dx_0 \sum_n$. Summation over double indices, e.g., $i = 1, 2$, is implied. \mathcal{T}_C denotes time ordering of the exponential integral along the closed time path \mathcal{C} which extends from the initial time $x_0=0$ to the largest relevant time in the functional integral and back to $x_0=0$, i.e., our short hand notation means

$$\int_{x,C} = \int_C dx_0 \sum_n = \left(\int_0^T dx_0 + \int_T^0 dx_0 \right) \sum_n. \quad (4)$$

Note that the closed-time contour can be seen as ensuring the normalization of the generating functional Z . The terms linear in the external fields J_i have been added to allow one to generate correlation functions of order n by functional differentiation:

$$\langle \mathcal{T}_C \hat{\Phi}(x_1) \cdots \hat{\Phi}(x_n) \rangle = \left. \frac{\delta^n Z[J, K; \hat{\rho}_D]}{i^n \delta J(x_1) \cdots \delta J(x_n)} \right|_{J=K=0}, \quad (5)$$

where the field indices have been suppressed. The fields K_{ij} are needed for the self-consistency condition of the two-point correlation functions as described below.

The generating functional (3) can be written, for Gaussian initial states, for which all correlation functions of order n

≥ 3 vanish at the initial time, as the functional integral (cf., e.g., [41])

$$Z[J, K] = \int \mathcal{D}\Phi \exp \left\{ i \left[S[\Phi] + \int_{x, \mathcal{C}} \Phi_i(x) J_i(x) + \frac{1}{2} \int_{xy, \mathcal{C}} \Phi_i(x) K_{ij}(x, y) \Phi_j(y) \right] \right\}. \quad (6)$$

Here,

$$S[\Phi] = \int_{xy, \mathcal{C}} \left[\frac{1}{2} \Phi_i(x) iD_{ij}^{-1}(x, y) \Phi_j(y) - \frac{U}{4\mathcal{N}} \delta_{\mathcal{C}}(x, y) \Phi_i(x) \Phi_i(x) \Phi_j(y) \Phi_j(y) \right] \quad (7)$$

is the classical action depending on the fluctuating fields Φ_i . The number of field components is $\mathcal{N}=2$, here. The delta function is defined as $\delta_{\mathcal{C}}(x, y) = \delta_{nm} \delta_{\mathcal{C}}(x_0 - y_0)$, with $x = (x_0, n)$, $y = (y_0, m)$. The classical inverse propagator reads

$$iD_{ij}^{-1}(x, y) = -i \delta_{\mathcal{C}}(x, y) \sigma_{2,ij} \partial_{y_0} - H_{1B}(x, y) \delta_{\mathcal{C}}(x_0 - y_0) \delta_{ij}, \quad (8)$$

where

$$H_{1B}(x, y) = -J(\delta_{n+1, m} + \delta_{n, m+1}) + \epsilon_n \delta_{nm} \quad (9)$$

is the one-body Hamiltonian. Note that the Gaussian initial conditions have been absorbed into the current terms by redefining the fields J and K accordingly [41].

B. Effective action and dynamic equations

In most situations the correlation functions up to order $n = 2$ are of primary interest, i.e., the mean field $\phi_i(x) = \langle \hat{\Phi}_i(x) \rangle$ and the normal and anomalous one-body density matrices, which, in the basis (2) relate to the diagonal ($i = j$) and off-diagonal ($i = 3 - j$) matrix elements of the two-point functions $G_{ij}(x, y) = \langle \mathcal{T}_{\mathcal{C}} \hat{\Phi}_i(x) \hat{\Phi}_j(y) \rangle_{\mathcal{C}}$, here generalized to unequal times $x_0 \neq y_0$ [42]. In Ref. [23] we have recalled the essential aspects of the 2PI (2-particle-irreducible) effective action approach which allows one in a transparent way to obtain equations of motion for these one- and two-point Green's functions within perturbative as well as nonperturbative approximation schemes with respect to the interaction constant U . We summarize the main results in the following.

Starting from the generating functional $Z[J, K] = \exp\{iW[J, K]\}$, Eq. (6), one derives, by double Legendre transform of the generating functional $W[J, K]$ of connected Green's functions, the 2PI effective action which is a functional of the one- and two-point functions [27–29]:

$$\Gamma[\phi, G] = S[\phi] + \frac{i}{2} \text{Tr} \{ \ln G^{-1} + G_0^{-1}[\phi] G \} + \Gamma_2[\phi, G] + \text{const.} \quad (10)$$

Here,

$$\begin{aligned} iG_{0,ij}^{-1}(x, y; \phi) &= \frac{\delta^2 S[\phi]}{\delta \phi_i(x) \delta \phi_j(y)} \\ &= \delta_{\mathcal{C}}(x_0 - y_0) \left(iD_{ij}^{-1}(x, y) - \frac{2U}{\mathcal{N}} [\phi_i(x) \phi_j(x) + \phi_k(x) \phi_k(x) \delta_{ij/2}] \delta_{nm} \right) \end{aligned} \quad (11)$$

is the classical inverse propagator, with $x = (x_0, n)$, $y = (y_0, m)$. $\Gamma[\phi, G]$ describes the quantum system completely, i.e., knowing it, one derives, by means of Hamilton's principle of stationary action,

$$\frac{\delta \Gamma[\phi, G]}{\delta \phi_i(x)} = 0, \quad \text{and} \quad \frac{\delta \Gamma[\phi, G]}{\delta G_{ij}(x, y)} = 0, \quad (12)$$

the exact many-body time evolution equations for ϕ and G .

As originally discussed in Refs. [27–29] $\Gamma_2[\phi, G]$ is represented as the sum of all closed two-particle irreducible (2PI) diagrams involving only the field ϕ , the full propagator G , and bare vertices $\propto U/\mathcal{N}$ [43]. To solve the dynamic equations approximations are made on the level of the effective action by truncating the diagrammatic expansion of $\Gamma_2[\phi, G]$. An important advantage of this approach is that crucial symmetries like total particle number, energy, momentum, angular momentum, etc., are automatically fulfilled irrespective of the particular truncation, cf., e.g., Ref. [23]. In the Appendix, we provide an explicit expression for the total energy within the NLO $1/\mathcal{N}$ approximation employed in this work.

The equations of motion resulting from Eqs. (12) are most conveniently written in terms of the real-valued statistical and spectral correlation functions,

$$F_{ij}(x, y) = \frac{1}{2} \langle \{ \hat{\Phi}_i(x), \hat{\Phi}_j(y) \} \rangle_{\mathcal{C}}, \quad (13)$$

$$\rho_{ij}(x, y) = i \langle [\hat{\Phi}_i(x), \hat{\Phi}_j(y)] \rangle_{\mathcal{C}}, \quad (14)$$

respectively. These are related to G through

$$G_{ij}(x, y) = F_{ij}(x, y) - \frac{i}{2} \rho_{ij}(x, y) \text{sgn}_{\mathcal{C}}(x_0 - y_0), \quad (15)$$

where $\text{sgn}_{\mathcal{C}}$ is the sign function which evaluates to 1 for $x_0 \geq y_0$ and to -1 otherwise. In this representation, the time ordering translates into time integration limits in the equations of motion:

$$\begin{aligned} & \left(-i \sigma_{2,ij} \partial_{x_0} - \frac{2U}{\mathcal{N}} F_{ij}(x, x) \right) \phi_j(x) - \int_{y, \mathcal{C}} \left(H_{1B}(x, y) \right. \\ & \left. + \frac{U}{\mathcal{N}} [\phi_k(x) \phi_k(x) + F_{kk}(x, x)] \delta_{\mathcal{C}}(x, y) \right) \phi_i(x) \\ & = \int_0^{x_0} dy \Sigma_{ij}^{\rho}(x, y; \phi \equiv 0) \phi_j(y), \end{aligned} \quad (16)$$

$$\begin{aligned}
& \int_{z,c} [-i\sigma_{2,ik}\delta_c(x,z)\partial_{z_0} - M_{ik}(x,z)] \begin{pmatrix} F_{kj}(z,y) \\ \rho_{kj}(z,y) \end{pmatrix} \\
&= \int_0^{x_0} dz \Sigma_{ik}^p(x,z;\phi) \begin{pmatrix} F_{kj}(z,y) \\ \rho_{kj}(z,y) \end{pmatrix} \\
& - \int_0^{y_0} dz \begin{pmatrix} \Sigma_{ik}^F(x,z;\phi) \\ \Sigma_{ik}^p(x,z;\phi) \end{pmatrix} \rho_{kj}(z,y). \quad (17)
\end{aligned}$$

Here,

$$\begin{aligned}
M_{ij}(x,y) &= \delta_{ij} \left[H_{1B}(x,y) + \frac{U}{\mathcal{N}} (\phi_k(x)\phi_k(x) + F_{kk}(x,x)) \delta_c(x,y) \right] \\
& + \frac{2U}{\mathcal{N}} (\phi_i(x)\phi_j(x) + F_{ij}(x,x)) \delta_c(x,y) \quad (18)
\end{aligned}$$

is the mean-field energy matrix which includes the ϕ_i -dependent terms of the classical inverse propagator $iG_{0,ij}^{-1}$, Eq. (11), and the local part $\Sigma_{ij}^{(0)}(x)$ of the self-energy

$$\Sigma_{ij}(x,y;\phi) = 2i \frac{\delta\Gamma_2[\phi,G]}{\delta G_{ij}(x,y)} \quad (19)$$

which, to derive the above equations, has been decomposed into real and imaginary parts as $\Sigma_{ij}(x,y;\phi) = \Sigma_{ij}^{(0)}(x)\delta_c(x,y) + \Sigma_{ij}^F(x,y;\phi) - (i/2)\Sigma_{ij}^p(x,y;\phi)\text{sgn}_c(x_0 - y_0)$ [23].

We point out that, neglecting the right-hand sides of Eqs. (16) and (17), these equations constitute a set of time-dependent Hartree-Fock-Bogoliubov (HFB) equations for the mean field and the two-point functions, cf., e.g., Refs. [22,23]. In this approximation, the dynamics of ρ decouples from that of ϕ and F . Neglecting also F , Eq. (16) is the Gross-Pitaevskii equation. Given the exact self-energy Σ , Eqs. (16) and (17) are the exact equations for the field ϕ and the correlation functions F and ρ , respectively. Equation (17) is equivalent to the Schwinger-Dyson equation for the full Green's function G .

C. Nonperturbative $1/\mathcal{N}$ approximation

To derive the quantum many-body time evolution, details about the self-energy Σ are required, and these are, in general, only available to a certain approximation. In the following we will consider an expansion of Γ_2 , to next-to-leading order (NLO) in powers of the inverse number of field components \mathcal{N} [19,30,44] which, in our special case, is $\mathcal{N}=2$. In the context of a nonrelativistic Bose gas, this approximation has been discussed in detail in Ref. [23]. The contribution $\Gamma_2[\phi,G]$ to the effective action Γ , Eq. (10), then involves a leading order (LO) and next-to-leading order (NLO) part which can be diagrammatically represented as shown in Fig. 1. While the leading-order contribution involves one diagram, in NLO a chain of bubble diagrams is resummed. All of these diagrams are proportional to the same power of $1/\mathcal{N}$ since each vertex scales with $1/\mathcal{N}$, which is cancelled by the (blue) propagator loops which scale with \mathcal{N} since they involve a summation over the field indices from 1 to \mathcal{N} . Note that the Hartree-Fock-Bogoliubov (HFB) approximation is given by an action Γ_2 which involves Γ_2^{LO} and the first dia-

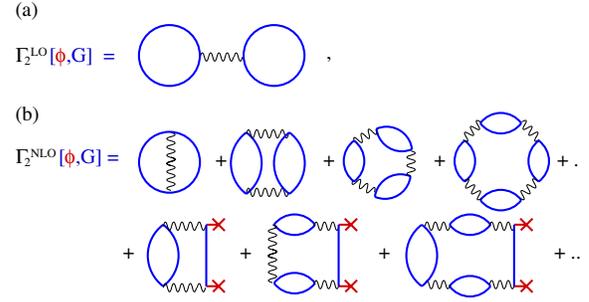


FIG. 1. (Color online) Diagrammatic representation of the leading order (LO) and next-to-leading order (NLO) contributions in the $1/\mathcal{N}$ expansion, to the 2PI part $\Gamma_2[\phi,G]$ of the 2PI effective action. The thick blue lines represent two-point functions $G_{ij}(x,y)$, the red crosses field insertions $\phi_i(x)$, and the wiggly lines vertices $U\delta_c(x,y)$. At each vertex, it is summed over double field indices i and integrated/summed over double time and space variables x .

gram of Γ_2^{NLO} in Fig. 1(b), cf., e.g., [23]. We compare, in the next section, our results in NLO of the $1/\mathcal{N}$ approximation with the HFB dynamics as well as with a perturbatively [45] reduced $1/\mathcal{N}$ approximation, the second-order coupling expansion, which, besides the HFB diagrams, takes into account still the two diagrams of second order in U , i.e., the second and fifth diagrams in Fig. 1(b), which contain two wiggly lines each.

From $\Gamma_2[\phi,G] = \Gamma_2^{\text{LO}}[\phi,G] + \Gamma_2^{\text{NLO}}[\phi,G]$ we obtain, using Eq. (19), the self-energies $\Sigma_{ij}(x,y) = \Sigma_{ij}^F(x,y) - (i/2)\text{sgn}_c(x_0 - y_0)\Sigma_{ij}^p(x,y)$, with

$$\begin{aligned}
\begin{pmatrix} \Sigma_{ij}^F(x,y) \\ -\frac{1}{2}\Sigma_{ij}^p(x,y) \end{pmatrix} &= -\frac{2U}{\mathcal{N}} \begin{pmatrix} I_F(x,y) \\ -\frac{1}{2}I_\rho(x,y) \end{pmatrix} \phi_i(x)\phi_j(y) \\
& + \begin{pmatrix} \Delta_F(x,y) & \frac{1}{2}\Delta_\rho(x,y) \\ -\frac{1}{2}\Delta_\rho(x,y) & \Delta_F(x,y) \end{pmatrix} \\
& \times \begin{pmatrix} F_{ij}(x,y) \\ -\frac{1}{2}\rho_{ij}(x,y) \end{pmatrix}, \quad (20)
\end{aligned}$$

where $\Delta_{F,\rho}(x,y) = I_{F,\rho}(x,y) + P_{F,\rho}(x,y;I_{F,\rho})$. The resummation to NLO in $1/\mathcal{N}$ is expressed by the coupled integral equations for $I_{F,\rho}$ [44,46]:

$$\begin{aligned}
\begin{pmatrix} I_F(x,y) \\ I_\rho(x,y) \end{pmatrix} &= \frac{U}{\mathcal{N}} \begin{pmatrix} F(x,y)^2 - \frac{1}{4}\rho(x,y)^2 \\ 2F_{ij}(x,y)\rho_{ij}(x,y) \end{pmatrix} \\
& - \int_0^{x_0} dz I_\rho(x,z) \begin{pmatrix} F(z,y)^2 - \frac{1}{4}\rho(z,y)^2 \\ 2F_{ij}(z,y)\rho_{ij}(z,y) \end{pmatrix} \\
& + \int_0^{y_0} dz \begin{pmatrix} I_F(x,z) \\ I_\rho(x,z) \end{pmatrix} 2F_{ij}(z,y)\rho_{ij}(z,y). \quad (21)
\end{aligned}$$

Here, $F^2 = F_{ij}F_{ij}$, etc. The functions $P_{F,\rho}$, which contribute to $\Delta_{F,\rho}$ in the self-energies (20) and vanish if $\phi_i \equiv 0$, read [44]

$$P_F(x,y;I_{F,\rho}) = -\frac{2U}{\mathcal{N}} \left\{ H_F(x,y) + \int_0^{y_0} dz [H_F(x,z)I_\rho(z,y) + I_F(x,z)H_\rho(z,y)] - \int_0^{x_0} dz [H_\rho(x,z)I_F(z,y) + I_\rho(x,z)H_F(z,y)] - \int_0^{x_0} dv \int_0^{y_0} dw I_\rho(x,v)H_F(v,w)I_\rho(w,y) + \int_0^{x_0} dv \int_0^{y_0} dw I_\rho(x,v)H_\rho(v,w)I_F(w,y) + \int_0^{y_0} dv \int_0^{y_0} dw I_F(x,v)H_\rho(v,w)I_\rho(w,y) \right\}, \quad (22)$$

$$P_\rho(x,y;I_{F,\rho}) = -\frac{2U}{\mathcal{N}} \left\{ H_\rho(x,y) - \int_{y_0}^{x_0} dz [H_\rho(x,z)I_\rho(z,y) + I_\rho(x,z)H_\rho(z,y)] + \int_{y_0}^{x_0} dv \int_{y_0}^{y_0} dw I_\rho(x,v)H_\rho(v,w)I_\rho(w,y) \right\}, \quad (23)$$

wherein the functions $H_{F,\rho}$ are defined as

$$H_F(x,y) = -\phi_i(x)F_{ij}(x,y)\phi_j(y), \quad (24)$$

$$H_\rho(x,y) = -\phi_i(x)\rho_{ij}(x,y)\phi_j(y).$$

The technical procedure to solve the above dynamic equations in every time step requires the determination of the functions $I(x,y)$ before the actual propagation of the respective correlation functions.

III. FAR-FROM-EQUILIBRIUM TIME EVOLUTION OF A ONE-DIMENSIONAL LATTICE BOSE GAS

A. Initial conditions

In the following we present our results for the time evolution of a lattice Bose gas initially in a state far from equilibrium. The 2PI approach invoked in this work allows us to specify initial states which are Gaussian in the sense that only the mean field and two-point correlation functions are nonzero at the initial time $t_0=0$. Note that, using a general n PI approach [41], also initial states with higher-order correlations can be taken into account.

The total number of particles $N_{\text{tot},n}(t)$ at lattice site n and time t is given as the sum of the number of condensed and excited atoms [$x=(t,n)$]:

$$N_{\text{tot},n}(t) = \langle \hat{\Psi}^\dagger(x)\hat{\Psi}(x) \rangle = N_{c,n}(t) + N_{\text{exc},n}(t), \quad (25)$$

$$N_{c,n}(t) = \frac{1}{2}[\phi_i(x)\phi_i(x)], \quad (26)$$

$$N_{\text{exc},n}(t) = \frac{1}{2}[F_{ii}(x,x) - 1], \quad (27)$$

where the constant -1 inside the parentheses takes into account the zero-point fluctuations. Formally, this -1 originates from the spectral function ρ which, due to the Bose commutation relations, vanishes at equal times, except for

$$-\rho_{12}(x_0,n;x_0,m) = \rho_{21}(x_0,n;x_0,m) = \delta_{nm}. \quad (28)$$

By virtue of the 2PI effective-action approach, total particle number as well as total energy are exactly conserved in all approximations obtained by truncating the diagrammatic expansion of Γ_2 , cf. the Appendix.

We consider initial states where the normal and anomalous fluctuations are zero, i.e., all atoms are in the condensate:

$$\langle \hat{\Psi}^\dagger(x)\hat{\Psi}(y) \rangle_c = [F_{ii}(x,y) - \delta_c(x,y)]/2 = 0,$$

and

$$\langle \hat{\Psi}(x)\hat{\Psi}(y) \rangle_c = [F_{11}(x,y) - F_{22}(x,y)]/2 + iF_{12}(x,y) = 0,$$

for $x_0=y_0=0$. Hence we choose

$$F_{11}(0,n;0,m) = F_{22}(0,n;0,m) = \delta_{nm}/2,$$

$$F_{12}(0,n;0,m) = F_{21}(0,n;0,m) = 0. \quad (29)$$

The initial values for ρ_{ij} are prescribed by Eq. (28). The condensate fraction is chosen to be nonzero at a single site m only,

$$\phi_j(0,n) = \sqrt{2N}\delta_{j1}\delta_{nm}, \quad (30)$$

where N is the total number of particles, and $j=1$ implies that the initial mean field $\psi = (\phi_1 + i\phi_2)/\sqrt{2}$ is real.

B. Numerical results

The expansion in inverse powers of the number of field components \mathcal{N} allows for approximations which are inherently nonperturbative, i.e., it takes into account diagrams up to infinite order in the physical coupling constant U . Dividing the equations of motion by the tunneling parameter J , neglecting quantum fluctuations [47], and taking into account that the $F_{ij}(x,y)$ and $\phi_i(x)\phi_j(y)$ approximately scale with the total number of particles N , one finds that all terms in the NLO $1/\mathcal{N}$ equations of motion (16) and (17) scale with some power of NU/J . In the series representing the self-energy Σ_{ij} , arbitrary high powers are resummed. The remaining terms which take into account the quantum fluctuations [48] are reduced by powers of N since the spectral functions $\rho_{ij}(x,y)$ are of order one. Nevertheless, if $NU/J > 1$ one expects that any perturbative or loop approximation of Γ_2 , neglecting terms with higher powers of NU/J , fails. In

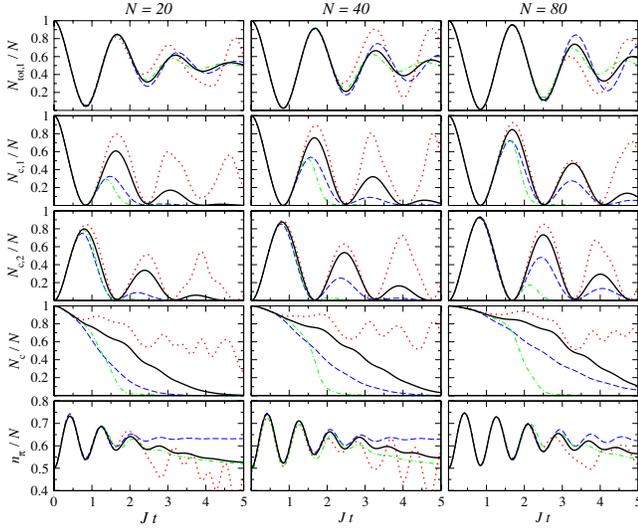


FIG. 2. (Color online) Time evolution of an ultracold Bose gas in a one-dimensional lattice with $N_L=2$ lattice sites and periodic boundary conditions. The three columns show the same quantities, for a different total number of atoms $N=20, 40,$ and $80,$ respectively. U/J is chosen such that the characteristic interaction parameter is $NU/J=4$ throughout. Initially, all atoms are in a Bose-Einstein condensate at lattice site 1. The graphs in the first line show the total number of atoms $N_{\text{tot},1}$ at site 1, normalized to N . Due to number conservation, one has $N_{\text{tot},2}=N-N_{\text{tot},1}$. The second and third lines show the condensate fractions $N_{c,n}/N$ at sites $n=1, 2,$ and the fourth line adds these up, $N_c/N=\sum_n N_{c,n}/N$. The last line shows the occupation n_q of the quasimomentum $q=\nu\pi$ [in units of $1/\text{lattice spacing}$] (31), for $\nu=1,$ normalized to the total quasimomentum occupation $n_0+n_\pi=N$. Notice the different scale in the last line. Our results from the $1/N$ expansion to NLO are shown as a thick solid line. The (blue) dashed lines show the results from an exact calculation by Rey and co-workers, cf. Figs. 5 and 6 of Ref. [22]. The (green) dash-dotted curves show the dynamics resulting from a $1/N$ expansion in a perturbative second-order coupling approximation (see text), the (red) dotted curves correspond to the Hartree-Fock-Bogoliubov approximation. With both sets of curves we reproduce the respective results in [22].

order to probe the accuracy of the nonperturbative $1/N$ approximation we chose NU/J to be larger than 1 and compare our results with the results of an exact numerical calculation [22] for limited numbers of lattice sites and particles. Following Ref. [22] we have considered cases with a total number of $N_L=2$ and $N_L=3$ lattice sites, and particle numbers between $N=8$ and 80 . Periodic boundary conditions were imposed. In Figs. 2 and 3 we present our results for the nonequilibrium quantum many-body evolution in the nonperturbative next-to-leading order (NLO) $1/N$ approximation as well as the ‘‘perturbative’’ Hartree-Fock-Bogoliubov (HFB) and second-order coupling approximations. In Fig. 2, we consider two lattice sites. The graphs in the first line show the total number of atoms $N_{\text{tot},1}$ at site 1, normalized to N . Due to number conservation, one has $N_{\text{tot},2}=N-N_{\text{tot},1}$. The second and third lines show the condensate fractions $N_{c,n}/N$ at sites $n=1, 2,$ cf. Eq. (26), and the fourth line adds these up, $N_c/N=\sum_n N_{c,n}/N$. The last line shows the occupation n_q of the quasimomentum $q_\nu=2\pi\nu/N_L,$ $\nu=1$ (q in units of $1/\text{lattice}$

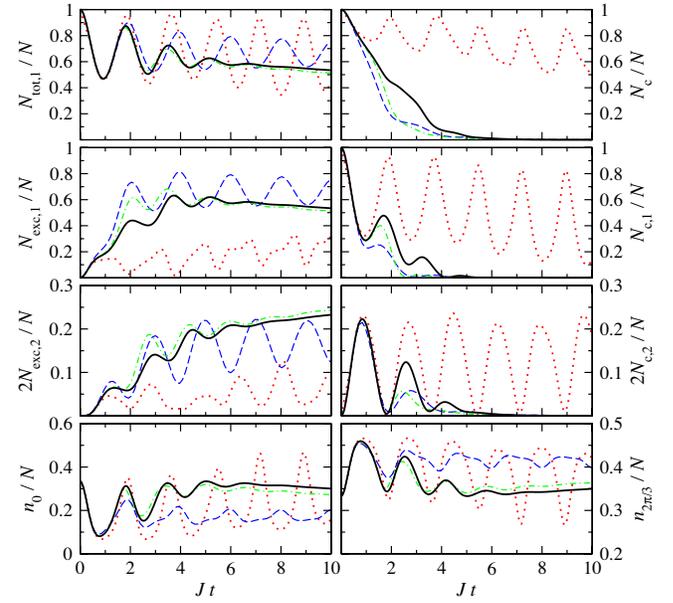


FIG. 3. (Color online) Time evolution of an ultracold Bose gas in a one-dimensional lattice with $N_L=3$ lattice sites and periodic boundary conditions. Only site $n=1$ is filled initially with $N=8$ atoms. The interaction strength is $U/J=1/3,$ such that $NU/J=2.67$. Besides the quantities already shown in Fig. 2, we show the depletion $N_{\text{exc},n}/N=(N_{\text{tot},n}-N_{c,n})/N$ at sites $n=1, 2.$ The populations of site $n=3$ are the same as those at $n=2$ due to the periodic boundary conditions. The curves indicate the same approximations as in Fig. 2. Notice the different scale in the third and fourth lines.

spacing), normalized to the total quasimomentum occupation $\sum_{\nu=0}^{N_L} n_{q_\nu}=N.$ n_q is defined as

$$\begin{aligned} n_q(t) &= \frac{1}{N_L} \sum_{nm} e^{iq(n-m)} \langle \Psi_n^\dagger(t) \Psi_m(t) \rangle \\ &= \frac{1}{2N_L} \sum_{nm} \{ \cos[q(n-m)] [F_{kk}(x,y) + \phi_k(x)\phi_k(y)] \\ &\quad + \sin[q(n-m)] [F_{21}(x,y) - F_{12}(x,y) \\ &\quad + \phi_2(x)\phi_1(y) - \phi_1(x)\phi_2(y)] - 1 \}, \end{aligned} \quad (31)$$

with $x=(t,n), y=(t,m).$ In Fig. 3, we consider three lattice sites, and plot the fractions of condensed, excited, and total atom numbers for sites 1 and 2, as well as the total number of condensed atoms $N_c=N_{c,1}+2N_{c,2}.$ We also plot the quasimomentum populations n_0 and $n_{2\pi/3}.$ Note that the respective populations of sites 2 and 3 are equal due to the periodic boundary conditions. For the quasimomentum populations this means that the term proportional to $\sin[q(n-m)]$ in Eq. (31) vanishes.

The solid line shows, in all plots, the evolution according to the dynamic equations in NLO $1/N$ approximation. For comparison, we show, as a dashed line, the results of an exact calculation obtained by Rey and co-workers for a coherent initial state of N atoms at one site [22].

The dotted and dash-dotted lines show the corresponding dynamics in the HFB and second-order coupling approxima-

tions, respectively, cf. Sec. II C. In the HFB approximation all nonlocal self-energy terms vanish in the equations of motion (16) and (17), and fluctuations enter in the form of a local energy shift only. This approximation is fully classical, i.e., it does not take into account any quantum statistical fluctuations, cf., e.g., Ref. [48] for a detailed discussion. In the second-order coupling expansion of the NLO $1/\mathcal{N}$ approximation, nonlocal contributions from the self-energy allow for damping. In Figs. 2 and 3, the dotted and dash-dotted lines precisely confirm the respective results of Ref. [22] for the HFB and second-order $1/\mathcal{N}$ approximations.

The time evolution shows different characteristic periods. At early times, the condensate oscillates coherently between the lattice wells. Only a small number of atoms is scattered from the condensate fraction into excited modes. This dynamics is effectively described by a set of coupled nonlinear Gross-Pitaevskii-like equations for the condensate mean field at the different lattice sites. These have the form of coupled single-particle Schrödinger equations, and the dynamics corresponds to Rabi oscillations. The frequency of these oscillations is determined by the expansion parameter NU/J . In the case of two lattice wells, the Bose-Hubbard lattice gas with periodic boundary conditions resembles a Josephson junction with coupling energy $E_J=2JN$, and charging energy $E_c=2U$, cf., e.g., [49,50]. For vanishing U , the system undergoes Rabi oscillations with frequency $\Omega=2E_J/N=4J$, i.e., the period of these oscillations is $T=(\pi/2)J^{-1}$. Note also that the choice of parameters $NU/J=4$, $N^2>400$ sets the system into the Josephson regime $N^{-2}(NU/J)\ll(NU/J)\ll N^2$. In this regime, the equilibrium state has a well-defined relative phase between the sites, and small oscillations around this configuration can be described as a collective excitation, the Josephson plasmon with plasma frequency $\omega_{JP}=\sqrt{E_J(E_c+4E_J/N^2)}=2J\sqrt{(NU/J)+4}$ [49]. We find, however, that the frequency of the large oscillations in Fig. 2 is closer to the Rabi frequency of an ideal gas than to the plasma frequency $\omega_{JP}=4\sqrt{2}J$, for which $T_{JP}\approx 0.35\pi/J$. This is, of course, not contradictory since the derivation of the above expression for ω_{JP} requires the assumption of small oscillations around equilibrium.

Due to the interactions between the atoms, also higher-order classical statistical and quantum correlations build up. To leading order this means that atoms are exchanged between the condensate and the noncondensate modes of the gas. These processes lead to a rapid destruction of the condensate fraction. Hence the coherence of the gas deteriorates which, on a somewhat longer time scale, leads to damping of the Rabi oscillations.

All three approximations describe the dynamics well within the first period of coherent oscillations. This was expected since the system is initially mostly classical, with higher-order correlations and fluctuations playing a minor role. At larger times, all approximations fail to describe the dynamics accurately. While the purely classical HFB approximation even qualitatively fails to show the correct damping behavior, the higher-order approximations yield damping but quantitatively different results. Our comparisons for different atom numbers N indicate that the accuracy of the NLO $1/\mathcal{N}$ approximation improves with increasing N . All examples show that the condensate fraction is, at large

times, underestimated in the second-order coupling expansion. Although it is overestimated in the NLO $1/\mathcal{N}$ approximation, our results show that the nonperturbative $1/\mathcal{N}$ resummation is capable of taking into account high correlations which, at large times, become relevant.

IV. CONCLUSIONS AND OUTLOOK

In this work we have studied the far-from-equilibrium dynamics of an ultracold, strongly interacting one-dimensional lattice Bose gas on the basis of the 2PI effective action in a next-to-leading-order (NLO) $1/\mathcal{N}$ approximation. The 2PI effective action preserves, at any truncation, vital conservation laws as total particle number and energy, and allows one to derive in a consistent way nonperturbative approximations which remain applicable also for strong interactions. For weakly interacting systems close to equilibrium, the 2PI approach gives the well-known mean-field theories and their kinetic extensions including the dynamics and dissipation of small excitations. However, the 2PI approach goes substantially beyond the basic Hartree-Fock-Bogoliubov approximation and leads to a description of dynamical evolution far from equilibrium in the form of an initial-value problem. Moreover, it is not restricted to a small number of particles.

The systems have been considered in the framework of the Bose-Hubbard model and consist of two and three lattice sites, one of which is coherently populated initially while the others are empty. Tunneling through the barriers leads to Rabi-like oscillations between the lattice wells which are damped due to particle interactions. We have studied the time evolution of the condensate and excited fractions of the gas as well as of the quasimomentum distribution and compared these results with those from the exact, fully quantal calculation of the dynamics from Ref. [22]. We find that in the nonperturbative $1/\mathcal{N}$ approximation the 2PI approach gives a reduced damping due to higher-order correlations as seen in the exact solution. Quantitatively, the damping of the oscillations of the condensate fractions is underestimated in the NLO $1/\mathcal{N}$ approximation while it is overestimated for the excited fractions. The agreement with the exact results appears to improve when choosing a larger total number N of particles. Our findings are similar to those in Ref. [36], where the nonequilibrium dynamics of a single nonlinear harmonic oscillator has been studied in the NLO as well as in a restricted NNLO $1/\mathcal{N}$ approximation and compared with the exact evolution. As compared to these results, which were obtained in the symmetric phase where the mean field ϕ vanishes, we do not find, in NLO $1/\mathcal{N}$, irregular behavior at large times, like the revivals seen in the Hartree-Fock-Bogoliubov approximation. A systematic study of the N -dependence of the accuracy of the $1/\mathcal{N}$ approximation, extending the exact studies to a larger particle number and lattice size, using, e.g., stochastic quantization techniques along the lines of [51], is the subject of ongoing work. We furthermore expect that the particular choice of an initial coherent-state population affects the ensuing damping behavior within the Markov time. This requires a detailed study of the non-Markovian effects which shall be a further topic of a future publication.

ACKNOWLEDGMENTS

We are very grateful to Jürgen Berges, Hrvoje Buljan, Markus Oberthaler, Michael G. Schmidt, Jörg Schmiedmayer, Gora Shlyapnikov, and Amichay Vardi for valuable discussions, and to Werner Wetzel for his continuing support concerning computing facilities. We would also like to thank Ana Maria Rey for allowing us to reproduce earlier results. This work has been supported by the Deutsche Forschungsgemeinschaft (T.G.).

APPENDIX: NUMBER AND ENERGY CONSERVATION

An important advantage of the 2PI effective action approach is that crucial symmetries like total particle number and energy are automatically fulfilled irrespective of the particular truncation. As was shown in Ref. [23] number conservation is a consequence of the Noether theorem in conjunction with the invariance of the theory under transformations which are elements of the group $O(\mathcal{N})$. Each 2PI diagram in the expansion of $\Gamma[\phi, G]$ separately carries this property such that any truncation of the series leads to number conservation. As a consequence, the total number

$$N(t) = \frac{1}{2} \int_{\vec{x}} [\phi_i(x) \phi_i(x) + G_{ii}(x, x)] \quad (\text{A1})$$

is conserved in time [23]. For the lattice gas, the spatial integral means $\int_{\vec{x}} f(x) = \sum_n f(t, n)$.

Energy conservation follows from time translation invariance of Γ , cf., e.g., Ref. [52]. Consider the general translations in continuous space and time which vanish at the boundary, $x^\mu \rightarrow x^\mu + \varepsilon^\mu(x)$, where $\varepsilon^\mu(x)$ is a time- and space-dependent infinitesimal four-vector. The mean field and two-point functions transform, under these translations, to leading order in ε , as $\phi_i(x) \rightarrow \phi_i(x) + \varepsilon^\nu(x) \partial_\nu^x \phi_i(x)$, and $G_{ij}(x, y) \rightarrow G_{ij}(x, y) + \varepsilon^\nu(x) \partial_\nu^x G_{ij}(x, y) + \varepsilon^\nu(y) \partial_\nu^y G_{ij}(x, y)$, respectively. Here, $\partial_\nu^x = \partial / \partial x^\nu$, etc. One can show that under these transformations the variation of the 2PI effective action Γ can be written as $\Gamma[\phi, G] \rightarrow \Gamma[\phi, G] + \delta\Gamma[\phi, G]$, with

$$\delta\Gamma[\phi, G] = \int_x T^{\mu\nu}(x) \partial_\mu^x \varepsilon_\nu(x). \quad (\text{A2})$$

Since, by virtue of the stationarity conditions (12), the variation $\delta\Gamma$ vanishes for all solutions of the equations of motion for ϕ_i and G_{ij} , an integration by parts shows that $T^{\mu\nu}$ is the conserved Noether current for the time-space translations:

$$\delta\Gamma[\phi, G] = - \int_x \varepsilon_\nu(x) \partial_\mu^x T^{\mu\nu}(x) = 0. \quad (\text{A3})$$

$T^{\mu\nu}(x)$ is identified as the energy-momentum tensor, and the conservation law for total energy is expressed as $\partial_\mu^x T^{\mu 0}(x) = 0$ or $\partial_t \int d^3x T^{00}(t, \vec{x}) = 0$.

To leading order in the $1/\mathcal{N}$ approximation we used the above space-time translations, and Eq. (A2), to derive the energy-momentum tensor. For the interaction terms which depend on the coupling U , however, as well as for the terms in NLO of the $1/\mathcal{N}$ approximation, it is more convenient to use a procedure known from field theory on curved space time. For a space-time-dependent metric $g_{\mu\nu}(x)$, the energy-momentum tensor is defined as [53]

$$T_{\mu\nu}(x) = \frac{2}{\sqrt{-g}} \frac{\delta\Gamma[\phi, G; g^{\mu\nu}]}{\delta g^{\mu\nu}}, \quad (\text{A4})$$

where $\sqrt{-g}$ denotes the square root of minus the determinant of $g_{\mu\nu}$.

In the following we only quote the result for the total energy $E(t) = \sum_n T_{00}(t, n)$ of the lattice Bose gas described by the Lagrangian (1). Using the above definitions and the useful relations $\delta g^{\mu\nu} = -g^{\mu\rho} g^{\nu\sigma} \delta g_{\rho\sigma}$ and $\delta \sqrt{-g} = \sqrt{-g} g^{\mu\nu} \delta g_{\mu\nu} / 2$, one obtains, in flat Minkowski space time, with $g^{\mu\nu} \equiv \text{diag}\{1, -1, -1, -1\}$:

$$\begin{aligned} E(t) = & \frac{1}{2} \int_{\vec{x}y} \delta_C(x, y) \left\{ H_{1B}(x, y) [\phi_i(y) \phi_i(x) + G_{ii}(y, x)] \right. \\ & + \frac{U}{\mathcal{N}} \left[\frac{1}{2} (\phi^2(x) + G_{ii}(x, x))^2 - 2H(x, x) \right] + I(x, x) \\ & \left. + \frac{2U}{\mathcal{N}} \left[2i \int_z H(x, z) I(x, z) + \int_{zu} I(x, z) H(z, u) I(u, x) \right] \right\}. \end{aligned} \quad (\text{A5})$$

Note that there is no integration over $x_0 = t$. Moreover, we use the definitions

$$I(x, y) = \frac{U}{\mathcal{N}} \left[G^2(x, y) - i \int_z I(x, z) G^2(z, y) \right], \quad (\text{A6})$$

$$H(x, y) = -\phi_i(x) G_{ij}(x, y) \phi_j(y), \quad (\text{A7})$$

with $G^2 = G_{ij} G_{ij}$. The term proportional to $[G_{ii}(x, x)]^2$ in Eq. (A5) stems from the LO contribution in the expansion of Γ_2 in powers of $1/\mathcal{N}$, and the term $I(x, x)$ as well as the last line from the NLO contributions, cf. Fig. 1.

[1] W. C. Stwalley, Phys. Rev. Lett. **37**, 1628 (1976).
 [2] E. Tiesinga, A. J. Moerdijk, B. J. Verhaar, and H. T. C. Stoof, Phys. Rev. A **46**, R1167 (1992).
 [3] S. Inouye, M. R. Andrews, J. Stenger, H.-J. Miesner, D. M. Stamper-Kurn, and W. Ketterle, Nature (London) **392**, 151 (1998).

[4] F. H. Mies, E. Tiesinga, and P. S. Julienne, Phys. Rev. A **61**, 022721 (2000).
 [5] E. A. Donley, N. R. Claussen, S. T. Thompson, and C. E. Wieman, Nature (London) **417**, 529 (2002).
 [6] D. Jaksch, C. Bruder, J. I. Cirac, C. W. Gardiner, and P. Zoller, Phys. Rev. Lett. **81**, 3108 (1998).

- [7] M. Greiner, O. Mandel, T. Esslinger, T. W. Hänsch, and I. Bloch, *Nature (London)* **415**, 39 (2002).
- [8] N. P. Proukakis and K. Burnett, *J. Res. Natl. Inst. Stand. Technol.* **101**, 457 (1996).
- [9] H. Shi and A. Griffin, *Phys. Rep.* **304**, 1 (1998).
- [10] C. W. Gardiner and P. Zoller, *Phys. Rev. A* **55**, 2902 (1997).
- [11] S. Giorgini, L. P. Pitaevskii, and S. Stringari, *Phys. Rev. Lett.* **78**, 3987 (1997).
- [12] N. P. Proukakis, K. Burnett, and H. T. C. Stoof, *Phys. Rev. A* **57**, 1230 (1998).
- [13] R. Walser, J. Williams, J. Cooper, and M. Holland, *Phys. Rev. A* **59**, 3878 (1999).
- [14] C. W. Gardiner and P. Zoller, *Phys. Rev. A* **61**, 033601 (2000).
- [15] R. Walser, J. Cooper, and M. Holland, *Phys. Rev. A* **63**, 013607 (2000).
- [16] A. M. Rey, B. L. Hu, E. Calzetta, and C. W. Clark, *Phys. Rev. A* **72**, 023604 (2005).
- [17] R. Baier and T. Stockamp, e-print hep-ph/0412310.
- [18] E. Calzetta and B. L. Hu, *Phys. Rev. D* **37**, 2878 (1988).
- [19] J. Berges, *Nucl. Phys. A* **699**, 847 (2002).
- [20] S. G. Bhongale, R. Walser, and M. J. Holland, *Phys. Rev. A* **66**, 043618 (2002).
- [21] T. Köhler and K. Burnett, *Phys. Rev. A* **65**, 033601 (2002).
- [22] A. M. Rey, B. L. Hu, E. Calzetta, A. Roura, and C. W. Clark, *Phys. Rev. A* **69**, 033610 (2004).
- [23] T. Gasenzer, J. Berges, M. G. Schmidt, and M. Seco, *Phys. Rev. A* **72**, 063604 (2005).
- [24] S. Peil, J. V. Porto, B. L. Tolra, J. M. Obrecht, B. E. King, M. Subbotin, S. L. Rolston, and W. D. Phillips, *Phys. Rev. A* **67**, 051603(R) (2003).
- [25] A. Polkovnikov, *Phys. Rev. A* **68**, 053604 (2003).
- [26] I. Tikhonenkov, J. R. Anglin, and A. Vardi, e-print cond-mat/0606609.
- [27] J. M. Luttinger and J. C. Ward, *Phys. Rev.* **118**, 1417 (1960).
- [28] G. Baym, *Phys. Rev.* **127**, 1391 (1962).
- [29] J. M. Cornwall, R. Jackiw, and E. Tomboulis, *Phys. Rev. D* **10**, 2428 (1974).
- [30] G. Aarts, D. Ahrensmeier, R. Baier, J. Berges, and J. Serreau, *Phys. Rev. D* **66**, 045008 (2002).
- [31] M. Alford, J. Berges, and J. M. Cheyne, *Phys. Rev. D* **70**, 125002 (2004).
- [32] J. Berges and J. Serreau, *Phys. Rev. Lett.* **91**, 111601 (2003).
- [33] B. Mihaila, J. F. Dawson, and F. Cooper, *Phys. Rev. D* **63**, 096003 (2001).
- [34] F. Cooper, J. F. Dawson, and B. Mihaila, *Phys. Rev. D* **67**, 056003 (2003).
- [35] A. Arrizabalaga, J. Smit, and A. Tranberg, *J. High Energy Phys.* **10** (2004) 017.
- [36] G. Aarts and A. Tranberg, *Phys. Rev. D* **74**, 025004 (2006).
- [37] G. Aarts and J. Berges, *Phys. Rev. D* **64**, 105010 (2001).
- [38] J. Berges, S. Borsányi, and J. Serreau, *Nucl. Phys. B* **B660**, 51 (2003).
- [39] J. Berges, S. Borsányi, and C. Wetterich, *Phys. Rev. Lett.* **93**, 142002 (2004).
- [40] G. Aarts and J. Berges, *Phys. Rev. Lett.* **88**, 041603 (2002).
- [41] J. Berges, *Phys. Rev. D* **70**, 105010 (2004).
- [42] The subscript c indicates that G is a connected Green's function or cumulant, $\langle \mathcal{T}_c \Phi_i(x) \Phi_j(y) \rangle_c = \langle \mathcal{T}_c \Phi_i(x) \Phi_j(y) \rangle - \phi_i(x) \phi_j(y)$.
- [43] In the context of condensed matter physics, a theory derivable from such an action functional is termed Φ -derivable.
- [44] J. Berges, e-print hep-ph/0409233; AIP Conf. Proc. No. 793 (AIP, New York, 2005), p. 3.
- [45] The term “perturbative” is used at the level of the 2PI effective action and therefore refers to a finite number of bare vertices in a certain 2PI diagram, irrespective of the inherently nonperturbative character of the self-consistently determined two-point functions.
- [46] Concerning Eqs. (B5)–(B8) and (B13) and (B14) of Ref. [23] an erratum is to be published.
- [47] It can be shown that quantum statistical fluctuations are taken into account by the ρ^2 terms in the functions $I_{F,\rho}$ as well as the $\Delta_\rho \rho_{ij}$ term in Σ_{ij}^F [48].
- [48] J. Berges and T. Gasenzer (unpublished).
- [49] G.-S. Paraoanu, S. Kohler, F. Sols, and A. J. Leggett, *J. Phys. B* **34**, 4689 (2001).
- [50] L. Pitaevskii and S. Stringari, *Phys. Rev. Lett.* **87**, 180402 (2001).
- [51] J. Berges and I.-O. Stamatescu, *Phys. Rev. Lett.* **95**, 202003 (2005).
- [52] A. Arrizabalaga, J. Smit, and A. Tranberg, *Phys. Rev. D* **72**, 025014 (2005).
- [53] C. W. Misner, K. S. Thorne, and J. A. Wheeler, *Gravitation* (Freeman, San Francisco, 1973).